Journal of AppliedMath 2025, 3(2), 2353.
https://doi.org/10.59400/jam2353

Article

Optimal control of dengue fever transmission dynamics in Kenya

Brian Nyanaro[1,*], George Kimathi[2], Mary Wainaina[1]

[1] Department of Mathematics and Actuarial Science, Catholic University of Eastern Africa, Nairobi 62157-00200, Kenya

[2] School of Computing and Information Technology, University of Kigali, Kigali 101, Rwanda

*** Corresponding author:** Brian Nyanaro, brian.nyanaro@gmail.com

CITATION

Nyanaro B, Kimathi G, Wainaina M. Optimal control of dengue fever transmission dynamics in Kenya. Journal of AppliedMath. 2025; 3(2): 2353. https://doi.org/10.59400/jam2353

ARTICLE INFO

Received: 23 December 2024
Accepted: 4 March 2025
Available online: 11 March 2025

Abstract: The emergence of dengue fever in Kenya has been witnessed in the recent past, leading to public health alerts and disruption of economic activities. The outbreaks have mainly been restricted to the Northeastern and Coastal counties of the country. As such, this paper has focused on an epidemiological model that incorporates an optimal control model of the spread dynamics of dengue fever in Kenya. The objective of the study is to develop an optimal control solution for the spread dynamics of dengue fever in Kenya. This study introduced three time-dependent control variables, which were divided into long-term and short-term control measures. The short-term control measures include prophylactics (treatment) and the use of physical barriers (nets), while the long-term control measure is the treatment of *Aedes aegypti* mosquitoes with Wolbachia bacteria. The basic reproduction number with the control variables was determined. The set of adjoint points of the control systems was obtained together with the optimal control set. The numerical solutions to the control problem were obtained by use of the forward-backward sweep method and the Runge-Kutta order four method. The impact of utilizing various strategies that employed the combination of the three control measures in different combinations was examined. The control profile of the particular control measures used was also investigated. It was determined that the short-term control measures had more impact on the control of the spread dynamics of dengue fever when compared to the long-term control measure. As such, it was determined that a strategy that incorporates both the long-term and short-term control measures should be utilized for optimum control of dengue fever spread dynamics in Kenya.

Keywords: adjoints; basic reproductive number; dengue fever; mathematical modelling; numerical simulations; optimal control; Pontrayagin's maximum principle; the Hamiltonian

1. Dengue fever in Kenya

In the recent past, dengue fever outbreaks in Kenya have become annual events due to various factors affecting the coastal region [1]. Such multifactorial contributing factors include increased population growth, increased urbanization, increased rapid movement of people from place to place, and climate change that favours increased activity of *Aedes Aegyti* and *Aedes albopictus* mosquitoes. These *Aedes Aegyti* and *Aedes albopictus* are the principal mosquitoes responsible for the spread of dengue fever in countries around the Indian Ocean [2].

The first reported cases of the latest outbreak of dengue fever were documented in January 2021 in the coastal counties of Lamu and Mombasa [3]. The initial cases had ballooned in Lamu County by April of the same year, indicating a high transmission rate of about 51% of the targeted sample of the community [4]. Immediate interventions were sought from the Red Cross Society through the Medical Services and Public Health Department of the county government of Lamu. Cases were on the rise in both counties, necessitating public health awareness across the two counties with more focus on Mvita sub-county, which accounted for a majority of the reported cases. However, the reported cases are not a true reflection of the transmission dynamics due to the high number of unreported cases and misdiagnoses that could have occurred [2]. These dynamics are discussed extensively in [1] and formed the basis of the optimal control problem studied in this publication.

Many studies have been conducted to examine the spread dynamics of dengue fever in Kenya using deterministic epidemiological modeling. However, there are few which have investigated the optimal control aspect of the managing the spread of dengue fever in Kenya [5]. In particular, this area of study is important due to resources scarcity experienced in the public health sector requiring high optimization of the available resources [6]. Furthermore, the funding scarcity presents an opportunity for exploration of less capital intensive control measures such as infection of mosquitoes with Wolbachia bacteria. In particular, the infection of mosquitoes with wolbachia bacteria is more Eco-friendly since it preserves the biodiversity of the mosquitoes [7,8]. As such, this study incorporated this approach of infecting mosquitoes with Wolbachia bacteria to the mathematics deterministic model discussed in [1]. The main objective of this study is to develop an optimal control solution of the spread dynamics of dengue fever using both analytical and numerical methods.

2. Model description and formulation

The model is divided into two broad subpopulations of vectors (Female *Aedes egypti* mosquitoes) and human beings. The female *Aedes egypti* mosquitoes will be divided into sub-populations as follows: Aquatic phase mosquitoes (eggs, larva, and pupa) $(L(t))$, Susceptible mosquitoes $(S_v(t))$, Exposed mosquitoes $(E_v(t))$, and Infectious mosquitoes $(I_v(t))$. The exposed compartment contains all mosquitoes that have been infected with dengue virus but are in the latent stage, where they are not infectious yet. Once a mosquito is infected with the dengue virus, it does not recover from it; it dies with the virus. The total population of the vectors is given by

$$N_v = L(t) + S_v(t) + E_v(t) + I_v(t)$$

The human subpopulation comprises the following compartments: the susceptible humans $(S_h(t))$, the exposed humans $(E_h(t))$, the infectious humans $(I_h(t))$, and the recovered $(R_h(t))$. The exposed humans are individuals already infected with dengue fever but in the latent stage before they become infectious. The recovered humans $(R_h(t))$ obtain temporary immunity from the serotype they have recovered from and a temporary immunity from the other three serotypes. The total population of the human beings is given by

$$N_h = S(t)_h + E_h(t) + I_h(t) + R_h(t)$$

2.1. Model formulation

The model subpopulations and their corresponding homogenous compartments are illustrated by the schematic representation in **Figure 1** below:

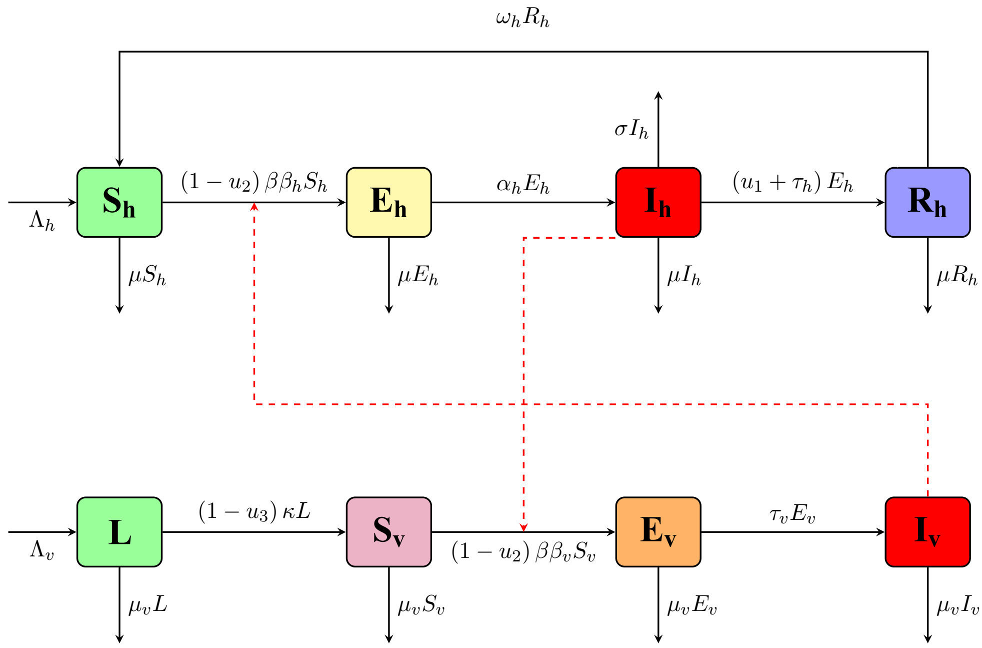

Figure 1. Dengue fever transmission dynamics model encompassing control parameters.

The pace of advancement from one compartment to another is quantified by the model parameters, which represent the illness development dynamics. The recruitment rate of the human subpopulation is denoted by Λ_h and it encompasses the natural birth rate as the dominating contributor. The recovery rate of human beings from one serotype is represented by τ_h, while the rate at which human temporary immunity wanes is represented by ω_h. The rate of infection of susceptible humans is represented by β_h, while the rate of human beings moving from the intrinsic incubation phase to the infectious phase is represented by α_h, while the natural death rate of human beings is represented by μ_h. Lastly, σ_h represents the disease-induced death. On the vector subpopulation, τ_v represents the rate at which vectors leave the extrinsic latent stage to become infectious. The egg-laying rate of *Aedes aegypti*, which dominates the recruitment rate of vector, is represented by Λ_v, while the survival rate of mosquitoes during the transition from pre-larvae to adults is represented by κ. β_v represents the infection rate of susceptible mosquitoes while the natural death rate of *Aedes aegypti* mosquitoes is represented by μ_v. A summary of the parameters that were considered for the study is presented in **Table 1** below.

Table 1. A summary of parameters, their values and sources.

Parameter	Description	Value (per day)	Source
Λ_h	Human Recruitment rate.	1538	[9]
τ_h	Human recovery rate.	0.154	[10]
ω_h	Immunity waning rate of humans.	0.1	Estimated
β_h	Infection rate of the susceptible Humans	4.8×10^{-8}	[11]
α_h	Rate of humans moving from latent stage to infectious stage.	0.12	[10]
σ_h	Dengue fever mortality rate	0.01969	[9]
μ_h	Natural death rate of humans.	0.0138214021	Calculated
τ_v	Rate of mosquitoes moving from latent stage to infectious stage	0.1	
Λ_v	Egg-laying rates of *Aedes aegypti* mosquitoes.	2938	[9]
κ	Survival rates of mosquitoes at the pre-development stage.	0.19	[10]
β_v	Infection rate of susceptible mosquitoes.	1×10^{-5}	[11]
μ_v	Natural death rate of *Aedes aegypti* mosquitoes.	0.0323	[10]

2.2. Model equations

The main objective of implementing optimal strategies in epidemiological models is to identify possible disease elimination strategies from the society. To achieve optimal control, we considered an elaborated dengue model with control variables. We proposed two Short-term control variables that included prophylactics (treatment) (u_1) and physical barriers (nets) (u_2) and one long-term control variable, treatment of *Aedes aegypti* mosquito eggs with Wolbachia bacteria (u_3). As a consequence, our system of non-linear differential equations changed to account for the introduced control variables. The system of differential equations is as follows:

$$\begin{cases} \dfrac{dS_h}{dt} = \Lambda_h - ((1-u_2)\,\beta\,\beta_h + \mu_h)\,S_h + \omega_h R_h \\ \dfrac{dE_h}{dt} = (1-u_2)\,\beta\,\beta_h\,S_h - (\alpha_h + \mu_h)\,E_h \\ \dfrac{dI_h}{dt} = \alpha_h\,E_h - ((u_1+\tau_h) + \mu_h + \sigma_h)\,I_h \\ \dfrac{dR_h}{dt} = (u_1+\tau_h)\;I_h - (\omega_h+\mu_h)\,R_h \\ \dfrac{dL}{dt} = \Lambda_v - ((1-u_3)\,\kappa + \mu_v)\,L \\ \dfrac{dS_v}{dt} = (1-u_3)\,\kappa L - ((1-u_2)\,\beta\,\beta_v + \mu_v)\,S_v \\ \dfrac{dE_v}{dt} = (1-u_2)\,\beta\,\beta_v\,S_v - (\tau_v+\mu_v)\,E_v \\ \dfrac{dI_v}{dt} = \tau_v\,E_v - \mu_v\,I_v \end{cases} \tag{1}$$

with initial conditions

$$S_h(0) \geqslant 0, E_h(0) \geqslant 0, I_h(0) \geqslant 0, R_h(0) \geqslant 0 S_v(0) \geqslant 0, E_v(0) \geqslant 0, I_v(0) \geqslant 0, R_v(0) \geqslant 0 \tag{2}$$

2.3. The basic reproduction number

The basic reproduction number of the system of differential Equation (1) was determined using the next generation matrix and established to be

$$\mathfrak{R}_1 = \frac{(\alpha_h \Lambda_h \mu_v \beta_h (\tau_v + \mu_v) \mu_v (\kappa + \mu_v) + \beta_2 \kappa \Lambda_v \tau_v (\alpha_h + \mu_h) (u_a + \tau_h + \mu_h + \sigma_h) \mu_h) (1 - u_b)}{\mu_v (\kappa + \mu_v) \mu_h \mu_v (\tau_v + \mu_v) (\alpha_h + \mu_h) (u_a + \tau_h + \mu_h + \sigma_h)} \quad (3)$$

2.4. Sensitivity analysis

Sensitivity analysis is conducted to determine the prominence of parameters contributing to the basic reproductive number ($\mathfrak{R}_1$), which consequently makes them the most significant drivers of the disease in the spread dynamics [12, 13]. In this study we considered the normalised forward-sensitivity index of the basic reproductive number $\mathfrak{R}_1$ with respect to a parameter x defined in Equation (4) [14].

$$\mathfrak{S}_x^{\mathfrak{R}_0} = \frac{x}{\mathfrak{R}_0} \cdot \frac{\partial \mathfrak{R}_0}{\partial x} \quad (4)$$

The numerical results of the local sensitivity indices calculated based on the basic reproductive number $\mathfrak{R}_1$ in Equation (3) using data in **Table 1** are summarised in the form of histograms, as shown in **Figure 2** below.

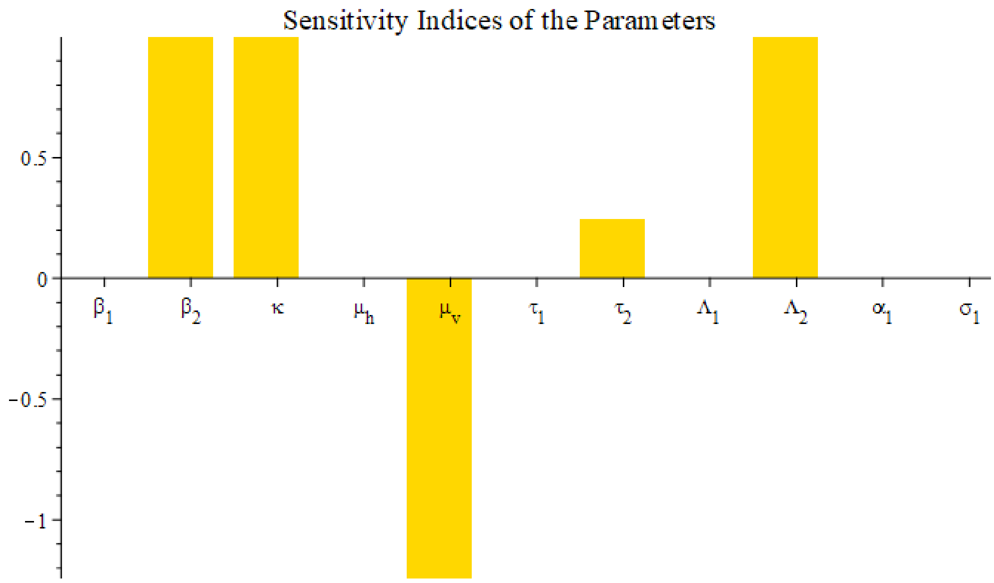

Figure 2. Sensitivity indices of parameters constituting the basic reproductive number.

As such, it was illustrated that the most sensitive parameters are β_v, which is the infection rate of susceptible mosquitoes, κ, which is the survival rate of mosquitoes at the pre-development stage, μ_v, which is the natural death rate of *Aedes Aegypti* mosquitoes, τ_h, which is the Rate of mosquitoes moving from latent stage to infectious stage, and Λ_v which is the egg-laying rate of *Aedes aegypti*. These parameters are the best targets for optimal control measures. However, this study focused on control measures that target the infection rate of susceptible mosquitoes, that is through physical barriers such as nets, and controlling the number of mosquitoes susceptible to dengue fever coming from the latent stage through infection with Wolbachia bacteria.

The optimal control measures are discussed in detail in Section 3 below.

3. Optimal control

The objective of this study is to minimize the number of dengue-infected vectors and hosts while managing the cost of implementing the controls u_1, u_2, and u_3 at their lowest possible levels. This objective can be summarized by the following objective functional

$$J(u_1,u_2,u_3) = \int_0^{t_f} \left(A_1 I_h + A_2 E_h + A_3 E_v + A_4 I_v + B_1 u_1^2 + B_2 u_2^2 + B_3 u_3^2\right) dt \tag{5}$$

Where the terms $B_1u_1^2$, $B_2u_2^2$, and $B_3u_3^2$ describe the cost incurred in administration of prophylactics, distribution of nets, and administration of Wolbachia bacteria, respectively.

The main aim will be to find the optimal control solution u_1^*, u_2^*, and u_3^* such that [9,15]

$$J\left(u_1^*, u_2^*, u_3^*\right) = \min_{u_1,u_2,u_3} \left\{J\left(u_1,u_2,u_3\right) : u_1,u_2,u_3 \in U\right\} \tag{6}$$

Where the control set of the optimal control problem is given by

$$U = \{u_1(t), u_2(t), u_3(t) : 0 \le u_1(t) \le 0.5, 0 \le u_2(t) \le 1, 0 \le u_3(t) \le 1, 0 \le t \le t_f, \}.$$

3.1. The Pontryagin's maximum principle

In order to establish the necessary condition for an optimal control problem, the Pontryagin's maximum principle was utilized [11, 16]. The principle converts the system of differential Equations (1)–(6) to a minimising point-wise problem with the Hamiltonian $\mathbb{H}$ with respect to $u_1, u_2,$ and u_3. The Hamiltonian $\mathbb{H}$ of the minimization problem is given by

$$\begin{aligned}\mathbb{H}\left(S_h,E_h,I_h,R_h,L,S_v,E_v,I_v,t\right) &= A_1 I_h + A_2 E_h + A_3 E_v + A_4 I_v + B_1 u_1^2 + B_2 u_2^2 + B_3 u_3^2 \\ &+ \lambda_1 \frac{dS_h}{dt} + \lambda_2 \frac{dE_h}{dt} + \lambda_3 \frac{dI_h}{dt} + \lambda_4 \frac{dR_h}{dt} + \lambda_5 \frac{dL}{dt} + \lambda_6 \frac{dS_v}{dt} + \lambda_7 \frac{dE_v}{dt} + \lambda_8 \frac{dI_v}{dt}\end{aligned}$$

which can be further expanded using Equation 1 to obtain

$$\begin{aligned}\mathbb{H}\left(S_h,E_h,I_h,R_h,L,S_v,E_v,I_v,t\right) &= A_1 I_h + A_2 E_h + A_3 E_v + A_4 I_v + B_1 u_1^2 + B_2 u_2^2 + B_3 u_3^2 \\ &+ \lambda_1 \left\{\Lambda_h - \left(\left(1-u_2\right)\beta\,\beta_h + \mu_h\right) S_h + \omega_h R_h\right\} + \lambda_2 \left\{\left(1-u_2\right)\beta\,\beta_h\, S_h - \left(\alpha_h + \mu_h\right) E_h\right\} \\ &+ \lambda_3 \left\{\alpha_h\, E_h - \left(\left(u_1 + \tau_h\right) + \mu_h + \sigma_h\right) I_h\right\} + \lambda_4 \left\{\left(u_1 + \tau_h\right)\, I_h - \left(\omega_h + \mu_h\right) R_h\right\} \\ &+ \lambda_5 \left\{\Lambda_v - \left(\left(1-u_3\right)\kappa + \mu_v\right) L\right\} + \lambda_6 \left\{\left(1-u_3\right)\kappa L - \left(\left(1-u_2\right)\beta\,\beta_v + \mu_v\right) S_v\right\} \\ &+ \lambda_7 \left\{\left(1-u_2\right)\beta\,\beta_v\, S_v - \left(\tau_v + \mu_v\right) E_v\right\} + \lambda_8 \left\{\tau_v\, E_v - \mu_v\, I_v\right\}\end{aligned}$$

in which the adjoint variables were given by $\lambda_1, \lambda_2, \lambda_3, \lambda_4, \lambda_5, \lambda_6, \lambda_7, \lambda_8$. The optimality condition requires that

$$\frac{d\lambda_i}{dt} = -\frac{\partial H}{\partial x(t)}$$

Where $x(t) = (S_h, E_h, I_h, R_h, L, S_v, E_v, I_v, t)$. As such, the partial differentiation of the Hamiltonian, $\mathbb{H}\left(S_h, E_h, I_h, R_h, L, S_v, E_v, I_v, t\right)$, with respect to $x(t) = (S_h, E_h, I_h, R_h, L, S_v, E_v, I_v, t)$ was obtained as shown below as follows:

$$\frac{d\lambda_1}{dt} = -\frac{\partial H}{\partial S_h} = -\beta\left(\lambda_1 - \lambda_2\right)\left(-1 + u_2\right)\beta_h + \mu_h\lambda_1 \tag{7}$$

$$\frac{d\lambda_2}{dt} = -\frac{\partial H}{\partial E_h} = \lambda_2\left(\alpha_h + \mu_h\right) - \lambda_3\alpha_h - A_2 \tag{8}$$

$$\frac{d\lambda_3}{dt} = -\frac{\partial H}{\partial I_h} = \left(u_1 + \tau_h + \mu_h + \sigma_h\right)\lambda_3 - \lambda_4\left(u_1 + \tau_h\right) - A_1 \tag{9}$$

$$\frac{d\lambda_4}{dt} = -\frac{\partial H}{\partial R_h} = \left(\omega_h + \mu_h\right)\lambda_4 - \lambda_1\omega_h \tag{10}$$

$$\frac{d\lambda_5}{dt} = -\frac{\partial H}{\partial L} = -\left(\lambda_5 - \lambda_6\right)\left(-1 + u_3\right)\kappa + \lambda_5\mu_v \tag{11}$$

$$\frac{d\lambda_6}{dt} = -\frac{\partial H}{\partial S_v} = -\lambda_6\left(\beta\left(u_2 - 1\right)\beta_v - \mu_v\right) \tag{12}$$

$$\frac{d\lambda_7}{dt} = -\frac{\partial H}{\partial E_v} = \left(\tau_v + \mu_v\right)\lambda_7 - \lambda_8\tau_v - A_3 \tag{13}$$

$$\frac{d\lambda_8}{dt} = -\frac{\partial H}{\partial I_v} = \lambda_8\mu_v - A_4 \tag{14}$$

The transversality condition for the above adjoint equations $\lambda_1, \lambda_2, \lambda_3, \lambda_4, \lambda_5, \lambda_6, \lambda_7,$ and λ_8 was determined to be

$$\lambda_1(T) = 0, \lambda_2(T) = 0, \lambda_3(T) = 0, \lambda_4(T) = 0, \lambda_5(T) = 0, \lambda_6(T) = 0, \lambda_7(T) = 0, \text{ and } \lambda_8(T) = 0$$

which guarantees the existence of an optimal control triple u_1^*, u_2^*, and u_3^* that justifies the functional $J\left(u_1^*, u_2^*, u_3^*\right) = \min_{u_1,u_2,u_3}\left\{J\left(u_1, u_2, u_3\right) : u_1, u_2, u_3 \in U\right\}$ in the control set U subject to the system of control differential Equation (1) and the initial conditions Equation (2). Characterising the optimal control was obtained by determining the solution to

$$\left.\frac{\partial \mathbb{H}}{\partial u_i}\right|_{u_i = u_i^*} = 0$$

Where $i = 1, 2, 3$ and u^* denotes the optimal control.

As such,

$$\begin{aligned} u_1^* &= \tfrac{I_h\left(\lambda_3 - \lambda_4\right)}{2B_1} \\ u_2^* &= \frac{\beta\left(S_h^{**}\left(\lambda_2 - \lambda_1\right)\beta_h - \lambda_6 S_{\mathrm{v}}^{**}\beta_v + \lambda_7 S_v^{**}\beta_v\right)}{2B_2} \\ u_3^* &= -\tfrac{L^{**}\left(\lambda_5 - \lambda_6\right)\kappa}{2B_3} \end{aligned}$$

Theorem 1. *Let's consider the state solution variables* $S_h^{**}, E_h^{**}, I_h^{**}, R_h^{**}, L^{**}, S_v^{**}$, E_v^{**}, *and* I_v^{**} *whose optimal control set is given by* $U^* = \left(u_1^*, u_2^*, u_3^*\right)$*, which are the control functions of the optimal control problem Equation* (1). The adjoint variables are given by $\lambda_1, \lambda_2, \lambda_3, \lambda_4, \lambda_5, \lambda_6, \lambda_7,$ and λ_8 which are the solutions of Equations

(7)–(14) respectively. The optimal control set (u_1^*, u_2^*, u_3^*) was given by

$$u_1^* = \max\left\{0,\ \min\left(0.5, \frac{I_h^{**}(\lambda_3-\lambda_4)}{2B_1}\right)\right\}$$
$$u_2^* = \max\left\{0,\ \min\left(1, \frac{\beta\left(S_h^{**}(\lambda_2-\lambda_1)\beta_h - \lambda_6 S_{\mathrm{v}}^{**}\beta_v + \lambda_7 S_v^{**}\beta_v\right)}{2B_2}\right)\right\}$$
$$u_3^* = \max\left\{0,\ \min\left(1, \frac{L^{**}(\lambda_5+\lambda_6)\kappa}{2B_3}\right)\right\}$$

Proof. The convexity of the integral of the functional $J(u_1^*, u_2^*, u_3^*)$ guarantees the existence of the optimal control of the 1 over the closed and convex control set $U^* = (u_1^*, u_2^*, u_3^*)$. The Lipschitz property of the state system is satisfied by the system Equation (1) due to the priori boundedness of the state solutions [16]. Where the boundedness is described by

$$u_1^* = \tilde{u}_1 = \frac{I_h^{**}(\lambda_3-\lambda_4)}{2B_1}$$
$$u_2^* = \tilde{u}_2 = \frac{\beta\left(S_h^{**}(\lambda_2-\lambda_1)\beta_h - \lambda_6 S_{\mathrm{v}}^{**}\beta_v + \lambda_7 S_v^{**}\beta_v\right)}{2B_2}$$
$$u_3^* = \tilde{u}_3 = \frac{L^{**}(\lambda_5+\lambda_6)\kappa}{2B_3}$$

which, by standard control argument, can be concluded to be as follows

$$u_1^* = \begin{cases} 0, & \text{if } \tilde{u}_1 \le 0 \\ \tilde{u}_1, & \text{if } 0 \le \tilde{u}_1 \le 0.5 \\ 1, & \text{if } \tilde{u}_1 \ge 0.5 \end{cases} \quad u_2^* = \begin{cases} 0, & \text{if } \tilde{u}_2 \le 0 \\ \tilde{u}_2, & \text{if } 0 \le \tilde{u}_2 \le 1 \\ 1, & \text{if } \tilde{u}_2 \ge 1 \end{cases} \quad u_3^* = \begin{cases} 0, & \text{if } \tilde{u}_3 \le 0 \\ \tilde{u}_3, & \text{if } 0 \le \tilde{u}_3 \le 1 \\ 1, & \text{if } \tilde{u}_3 \ge 1 \end{cases}$$

For sufficiently small-time intervals of simulations, convectional techniques can be used to the uniqueness of the optimal control system solution. In particular, this approach was utilised for this work because the right side of both the adjoint and the state variables are Lipschitz continuous. Furthermore, since the optimal control system is bounded, the adjoint system contains linear bounded coefficients; thus, the system of adjoints has upper bounds. The imposition of conditions that guarantee small time in the time interval, guarantees the uniqueness of the optimal control of the system [17]. The application of the small-time condition is because of the reverse time orientation of the optimal system, with the state problem having the initial values while the adjoint problem has the final times [18]. □

4. Numerical results

In this section, we present the graphical solution of the optimal control problem Equation (1) in comparison with the system of differential equations without the control parameters. The methods also employed the parameters detailed in **Table 1** above and the following initial conditions.

The initial conditions are taken from the seventieth day of the simulation without control measures. That is,

$$S_h(0) = 100000, \quad E_h(0) = 444, \quad I_h(0) = 313, \quad R_h(0) = 20,$$
$$L(0) = 13186, \quad S_v(0) = 37577, \quad E_v(0) = 6900, \quad I_v(0) = 24371.$$

In order to minimise the spread of dengue fever, the exposed populations and infectious populations of both human beings and mosquitoes needed to be minimised. The relative importance coefficients $A_1 = A_2 = A_3 = A_4 = 2$ of each of the four compartments to be minimised was assumed to be equal. The unit cost of treating dengue fever in Kenya was taken to be $B_1 = 2990$ [19], and the cost of nets as the primary physical barrier was taken to be $B_2 = 786$, which is the average cost of nets that cost between \$5 and \$7 [20], and the unit cost of infecting mosquitoes with Wolbachia bacteria was assumed to be $B_3 = 4494$ [21].

Based on the above numerical simulations, various economic strategies for optimal control were explored. These strategies included:

- **Strategy 1:** The combined utilization of physical barriers (bed nets) and treatment of pre-adult mosquitoes with Wolbachia bacteria, i.e., $u_1 = 0, u_2 \neq 0, u_3 \neq 0$.
- **Strategy 2:** The combined utilization of prophylactics and treatment of pre -adult mosquitoes with Wolbachia bacteria, i.e., $u_1 \neq 0, u_2 = 0, u_3 \neq 0$.
- **Strategy 3:** The combined utilization of prophylactics and Physical barriers (Nets), i.e., $u_1 \neq 0, u_2 \neq 0, u_3 = 0$.
- **Strategy 4 :** The combined utilization of prophylactics, physical barriers, and treatment of pre -adult mosquitoes with Wolbachia bacteria, i.e., $u_1 \neq 0, u_2 \neq 0, u_3 \neq 0$.

These strategies were further investigated as discussed below .

4.1. The combined utilization of physical barriers (bed nets) and treatment of pre -adult mosquitoes with Wolbachia bacteria, i.e., $u_1 = 0, u_2 \neq 0, u_3 \neq 0$

In this strategy, the susceptible human population increases slightly due to the decrease in the infection rate occasioned by the treatment of the pre-adult mosquitoes by Wolbachia bacteria, as illustrated in **Figure 3a**. The exposed human population decreases to near zero in the first 50 days of the implementation of the strategy, as illustrated in **Figure 3b**. The significant drop can be attributed to the compounding effect of the two control measures. **Figure 3c** illustrates the impact of the compounded effect of the two control measures that led to a significant drop in the infectious human population. Specifically, the infectious population reduced to near zero values in the first 80 days of the simulation with the strategy. As a consequence, the recovered human population under the strategy remained significantly lower when compared to when there are no control interventions, as illustrated in **Figure 3d**.

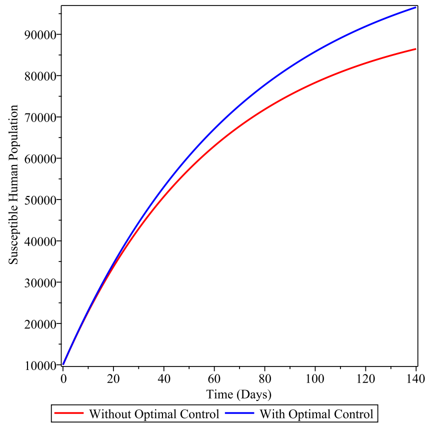

(a) Susceptible human population

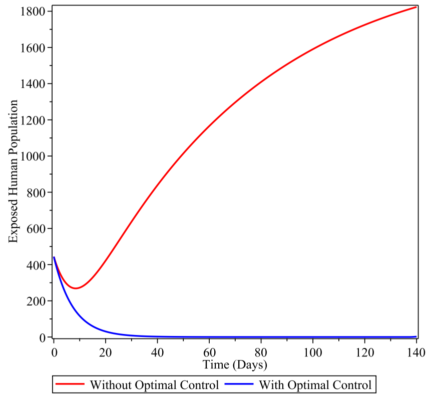

(b) Exposed human population

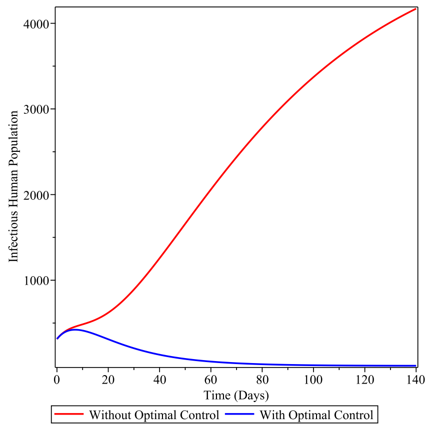

(c) Infectious human population

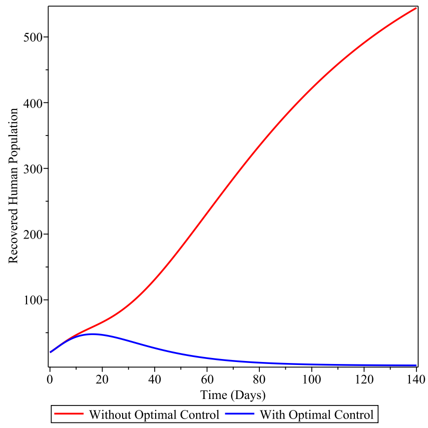

(d) Recovered human population

Figure 3. Comparative graphs of dengue spread dynamics in the human population under strategy 1 optimal control.

The mosquito population dynamics are also affected by the impact of the compound effect of the two control measures. The aquatic mosquito population remains fairly the same since the control measures do not include killing of mosquitoes, thus maintaining biodiversity as illustrated in **Figure 4a**. Specifically, this is a sustainable way to manage the spread of dengue fever. In **Figure 4b**, the susceptible mosquito population remained high because of the reduced susceptibility to dengue fever. This graph further emphasizes the impact of the control measures in ensuring the susceptible mosquitoes remain harmless by eradicating dengue virus instead of eradicating the mosquitoes. The exposed mosquito population reduced drastically to near zero in the first 50 days of implementing the control measures under this strategy, as illustrated in **Figure 4c**. The sustained low population of the exposed mosquito population is attributed to the compounding effect of the two control measures. By extension, the infectious mosquito population in **Figure 4d** has the same trend due to the same compounding effect of the strategy.

This strategy utilizes physical barriers in the form of nets (u_2) and treatment of the aquatic mosquito population with Wolbachia bacteria (u_3). The use nets should be sustained at 100% for 135 days of the simulation, then dropped sharply to zero in the remaining 5 days of the simulation, as illustrated in **Figure 5a**. At the same time, treatment with Wolbachia bacteria should continue at varying degrees on all the days of the simulation, as illustrated in **Figure 5b**.

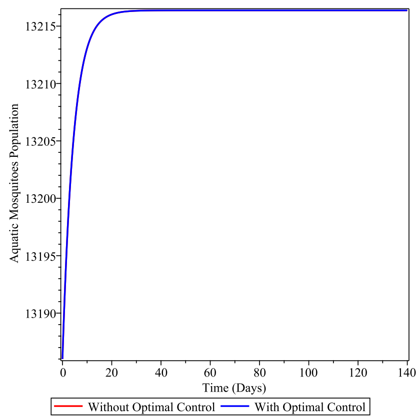

(a) Aquatic mosquito population

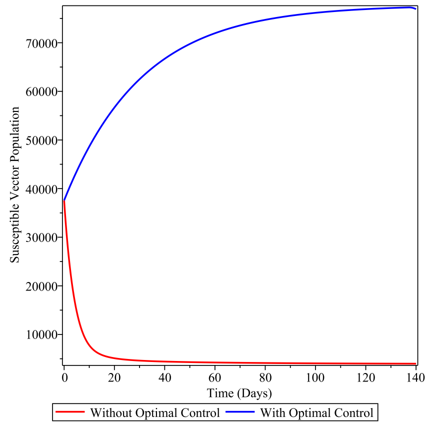

(b) Susceptible mosquito population

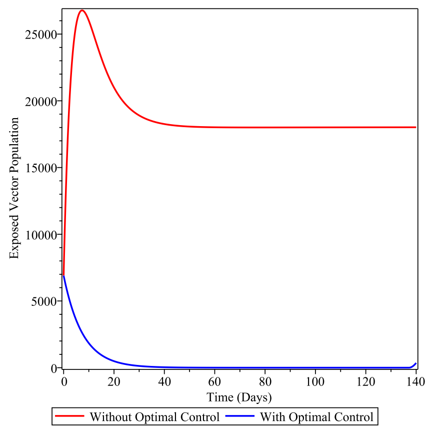

(c) Exposed mosquito population

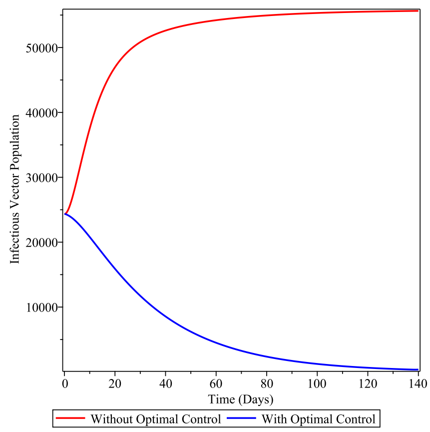

(d) Infectious mosquito population

Figure 4. Comparative graphs of dengue spread dynamics in the vector population under strategy 1 optimal control.

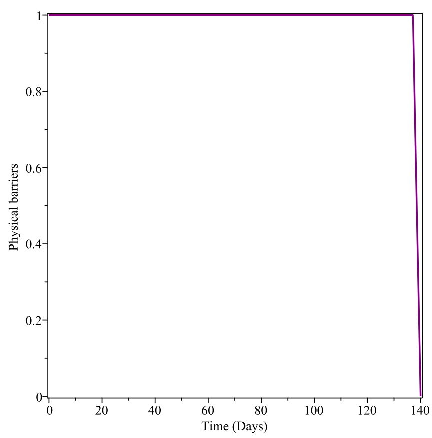

(a) Physical barriers (u_2)

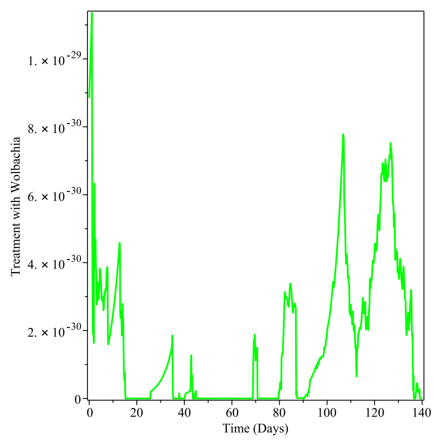

(b) Treatment with Wolbachia bacteria (u_3)

Figure 5. Control profiles of the control measures values applied in strategy 1.

4.2. The combined utilization of prophylactics and treatment of pre-adult mosquitoes with Wolbachia bacteria, i.e., $u_1 \neq 0, u_2 = 0, u_3 \neq 0$

In this strategy, the susceptible human population is slightly increased when compared to the dynamics without control measures, while the exposed population remain unchanged since both control measures do not target these compartment. From **Figure 6a** the infectious population is significantly lower after the implementation of the control measures when compared to the spread dynamics without control measures.

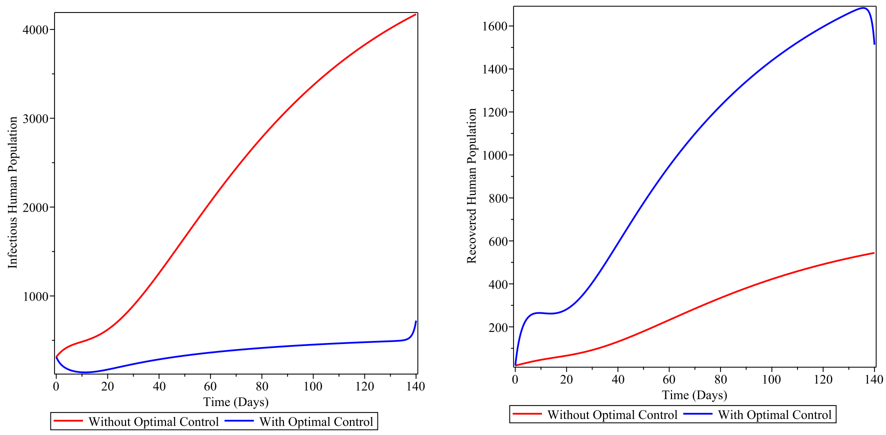

(a) Infectious human population **(b)** Recovered human population

Figure 6. Comparative graphs of dengue spread dynamics in the human population under strategy 2 optimal control.

The vector population dynamics are not affected by the utilization of this strategy since the utilization of prophylactics overshadows the infection of the pre-adult population with Wolbachia bacteria. As a consequence, the spread dynamics are more controlled by treating the infected human beings than focusing on containing the vector population. The vector populations remain the same before and after control measures.

This strategy entails the utilization of Prophylactics (u_1) and treatment of pre-adult mosquitoes with Wolbachia bacteria (u_3), which is a combination of a short-term control measure and a long-term control measure. Their application dynamics are illustrated in the **Figure 7a,b**, respectively. Prophylactics dominated this strategy since it is best suited for effective short-term management of diseases, leading to no contribution of treatment of pre-adult mosquitoes with Wolbachia bacteria.

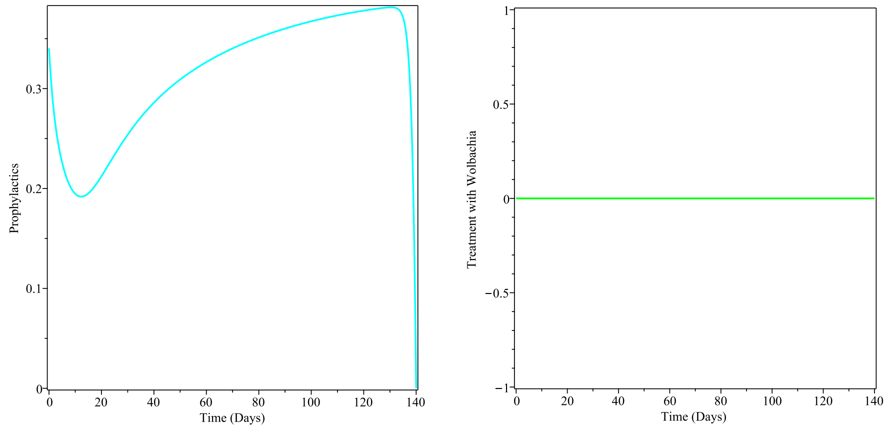

(a) Prophylactics (u_1)

(b) Treatment with Wolbachia bacteria (u_3)

Figure 7. Control profiles of the control measures values applied in strategy 2.

4.3. The combined utilization of prophylactics and physical barriers (Nets), i.e., $u_1 \neq 0, u_2 \neq 0, u_3 = 0$

This strategy has a small impact on the susceptible population. The exposed human population is reduced to near zero values in the first 30 days of implementing the control strategy, as illustrated in **Figure 8a**. The infectious human population is reduced to very low manageable levels within the first 30 days of implementing the control strategies as illustrated by **Figure 8b**.

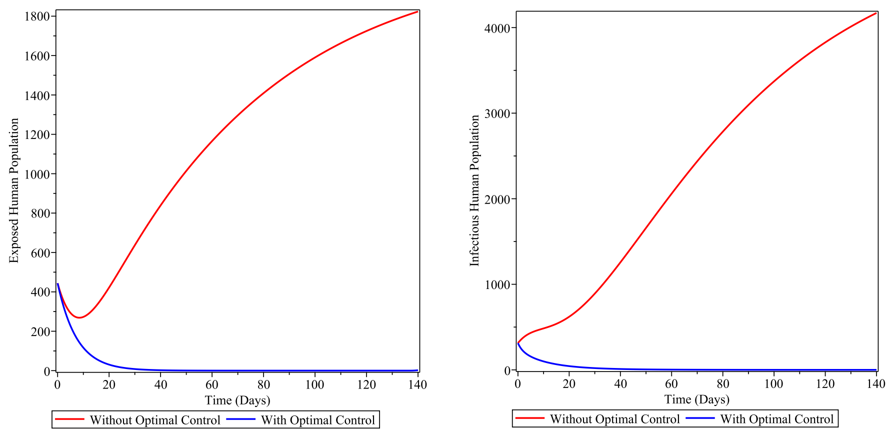

(a) Exposed human population

(b) Infectious human population

Figure 8. Comparative graphs of dengue spread dynamics in the human population under strategy 3 optimal control.

The vector population dynamics are impacted differently. The aquatic mosquito population is not affected by these two strategies, as shown by **Figure 9a**. The susceptible mosquitoes increase much more after the implementation of the control strategy when compared to before the implementation. These spread dynamics are illustrated in **Figure 9b**. In **Figure 9c**, the exposed vector population reduces to near zero level in the first 30 days of application of the control strategy. As a consequence, the infectious vector population also follows a similar trend but over a long period of time, as illustrated in **Figure 9d**. The population of the infectious mosquito population drops progressively to near zero levels in the 140 days of application of the control strategy, while the population of the infectious population increases in the absence of a control strategy. These dynamics are attributed to the compounding effect of the two control measures in this strategy.

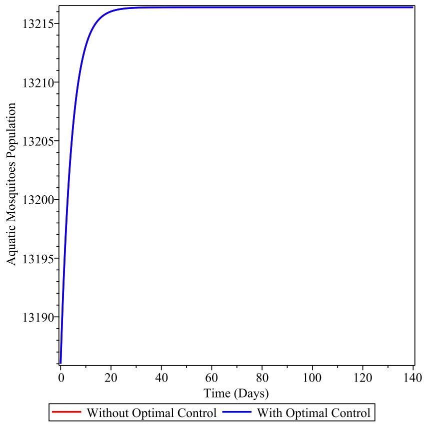

(a) Aquatic mosquito population

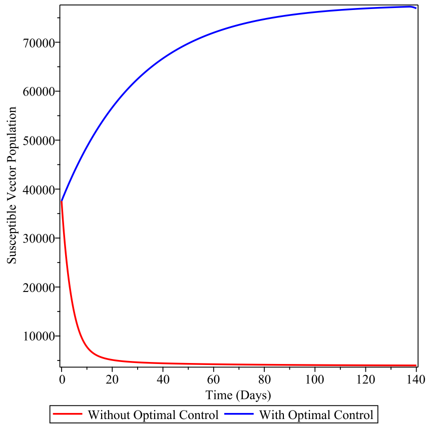

(b) Susceptible mosquito population

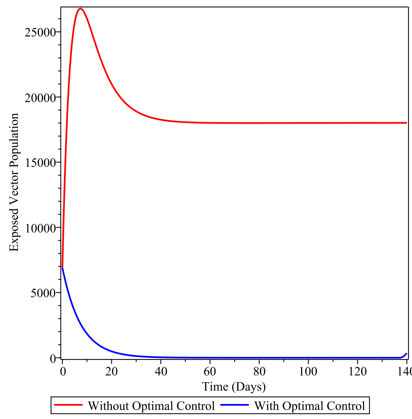

(c) Exposed mosquito population

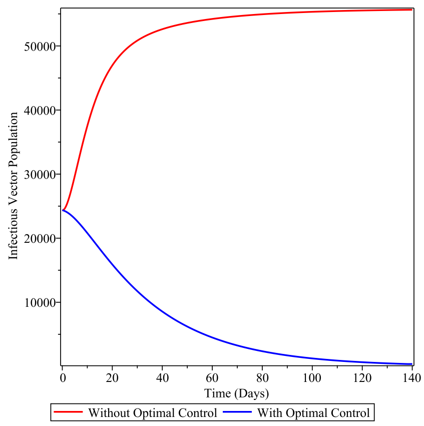

(d) Infectious mosquito population

Figure 9. Comparative graphs of dengue spread dynamics in the vector population under strategy 3 optimal control.

This strategy entailed the application of prophylactics (u_1) and physical barriers (u_2) in the control of dengue fever spread dynamics. The use of nets was utilized for the first 135 days out of the 140 days of the simulation, as illustrated in **Figure 10a**, and reduced progressively to zero in the last 5 days of the simulation. The prophylactics were applied following a decay graph, as indicated by **Figure 10b** . The decay graph is a result of the compounding impact of the two-control measure, which complement each other. The use of physical barriers prevents new infections, while the progressive application of prophylactics treats existing infectious individuals, leading to the progressive eradication of the disease.

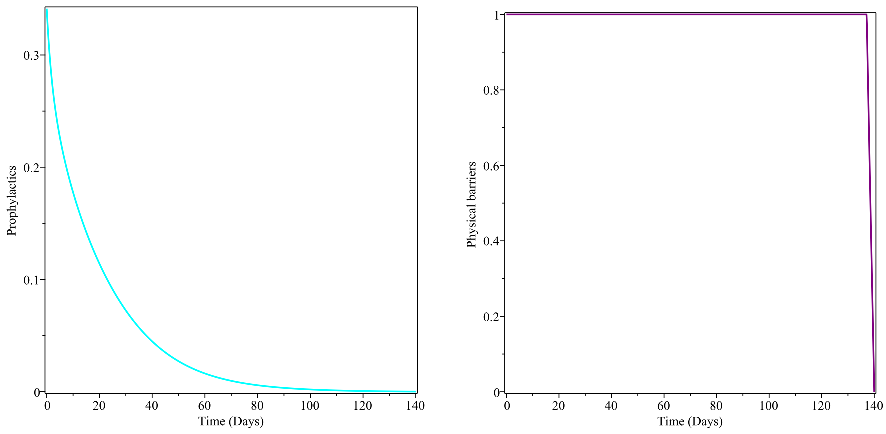

(a) Prophylactics (u_1)

(b) Physical barriers (u_2)

Figure 10. Control profiles of the control measures values applied in strategy 3.

4.4. The combined utilization of prophylactics, physical barriers, and treatment of pre -adult mosquitoes with Wolbachia bacteria, i.e., $u_1 \neq 0, u_2 \neq 0, u_3 \neq 0$

This strategy consists of a combination of all the control measures investigated in this study. The exposed human population drops drastically to near zero levels in the first 30 days of implementing this strategy, as shown in **Figure 11a**. As a result, the trend of the infectious human population is illustrated in **Figure 11b**. From the graph, the infectious population drops to near zero levels after the 30th day of applying the strategy.

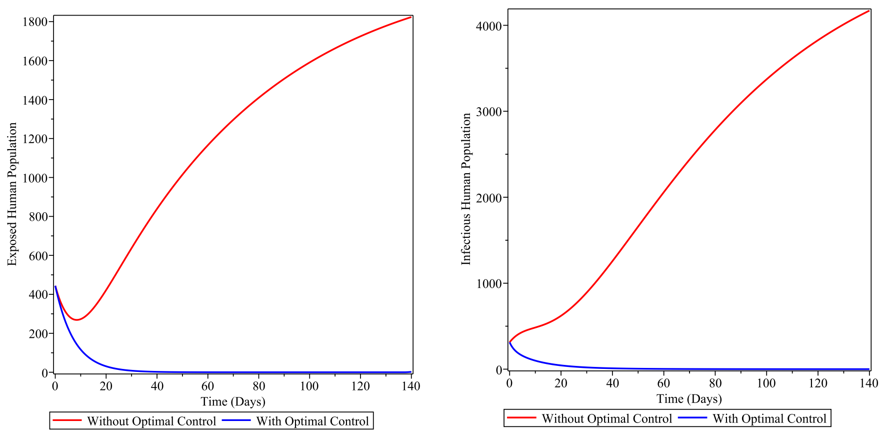

(a) Exposed human population

(b) Infectious human population

Figure 11. Comparative graphs of dengue spread dynamics in the human population under strategy 4 optimal control.

The aquatic mosquito population dynamics remain the same before and after the control measure strategies, as shown in **Figure 12a**, since the control measures do not target to reduce this population. This strategy was designed to preserve biodiversity by avoiding control measures that target killing of mosquitoes. The compounding impact of the three control measures leads to the susceptible mosquito population remaining very high after the application of the control strategy when compared to before the application of the control strategy, as shown in **Figure 12b**. The exposed mosquito population drops drastically to near zero levels after the first 50 days of the implementation of the control strategy, as illustrated in **Figure 12c**. As a consequence, the infectious vector population reduces progressively in the 140 days of the application of the strategy as illustrated in **Figure 12d**.

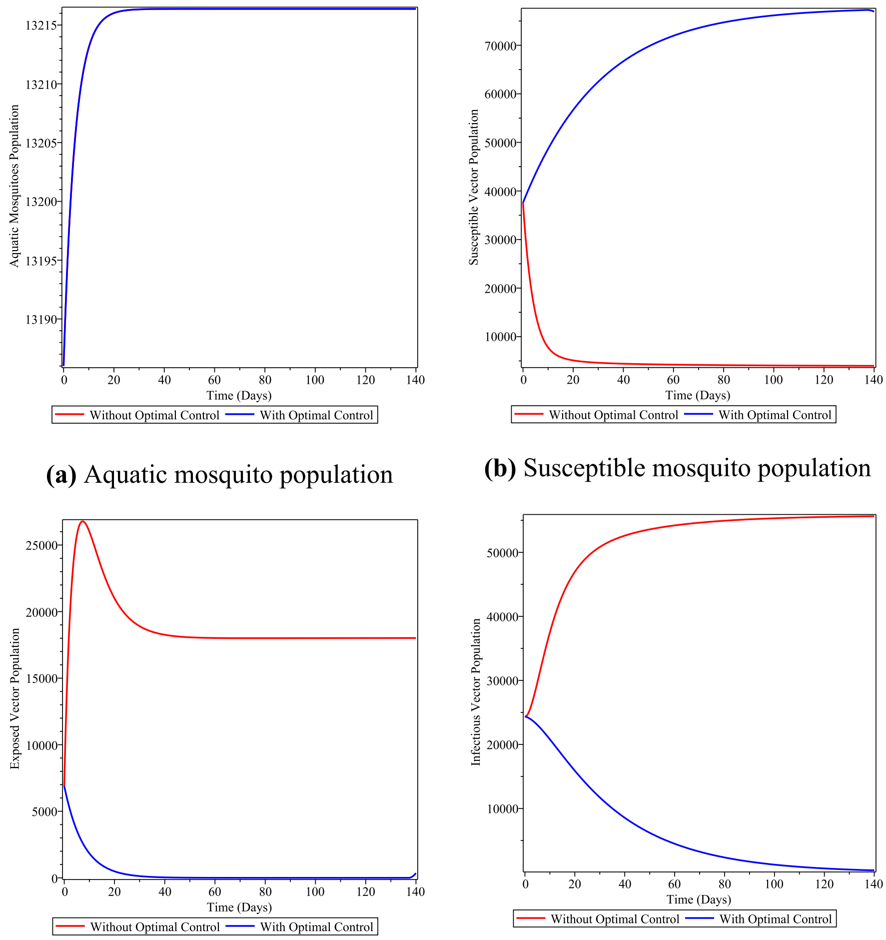

(a) Aquatic mosquito population

(b) Susceptible mosquito population

(c) Exposed mosquito population

(d) Infectious mosquito population

Figure 12. Comparative graphs of dengue spread dynamics in the vector population under strategy 4 optimal control.

This strategy involved the combination of all the control parameters of the study, that is, the two short-term control measures: Prophylactics (u_1) and the use of physical barriers such as nets (u_2), and the long-term control measure, which is treatment of pre-adult mosquitoes with Wolbachia bacteria (u_3). The control profiles of the control measures values are illustrated in **Figure 13a–c** above. These control profiles highlight the complementary application of the control measure to achieve a compounding effect on the control of dengue fever. The impact of the long-term control measure is very low since it takes a lot of time before the effectiveness of the control measures can be able to match the impact of the short-term control measures.

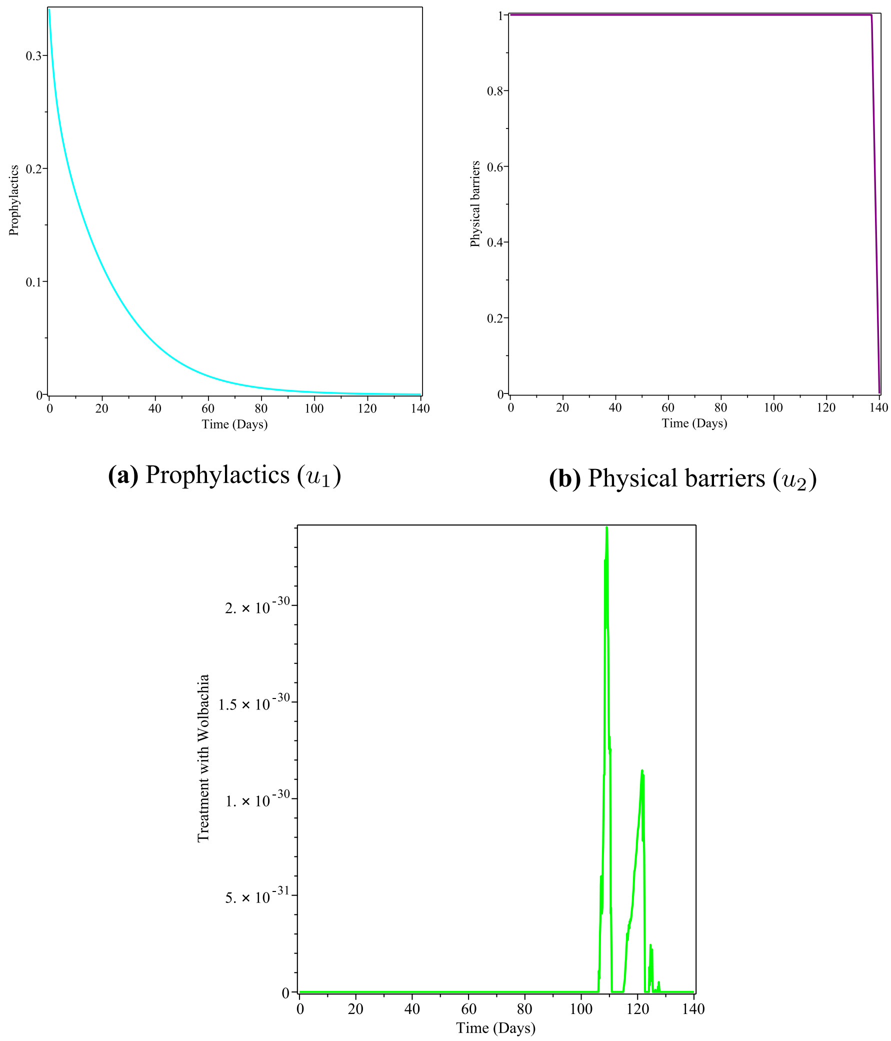

(a) Prophylactics (u_1)

(b) Physical barriers (u_2)

(c) Treatment with Wolbachia bacteria (u_3)

Figure 13. Control profiles of the control measures values applied in strategy 4.

5. Conclusions and recommendations

5.1. Conclusions

In conclusion, a modified deterministic model that incorporate the control parameters, that is, Prophylactics (u_1), the use of physical barriers such as nets (u_2), and treatment of pre-adult mosquitoes with Wolbachia bacteria (u_3) was developed. The arising non-linear differential equations were formulated and used to determine the basic reproduction number. The objective functional was developed by utilizing the control parameters. The necessary conditions for establishing the optimal control solutions were determined using the Pontryagin's maximum principle. The Hamiltonian of the minimizing problem was determined together with adjoints. A numerical analysis of the optimal control problem was done based on various strategies that combined the control measures. The output of the strategies was compared with output without the control measures. A comparative analysis of these graphs was done. It was determined that different combination of different control measures had different impacts on the various sub-populations in the compartments.

5.2. Limitations

This study was able to establish some key findings discussed in Section 5.1 above. However, there were some limitations associated with the study that would refine the study. Some of the limitations include lack of sufficient data on the spread dynamics in Kenya due to limited resources for health data management systems. The implementation of long-term strategies such as the infection of *Aedes aegypti* mosquitoes with wolbachia bacteria lack effective monitoring strategies thus its data is limited in scope. As such, if these limitations are addressed this study can be refined further to give more insights to the spread dynamics.

5.3. Recommendations

The study recommends that a cost-effective analysis of the strategies be conducted to determine the most cost-effective strategy for combating the spread of dengue fever in Kenya. The cost-effective analysis should also discuss economic feasibility of the strategies on a resource scarce state like Kenya. It also recommends further research on the impact of both short-term and long-term control measures on the overall management of dengue fever. Furthermore, more analytical studies can be conducted on the spread dynamics of dengue fever by carrying efficacy studies in scenarios where these strategies will be conducted. In addition, the study recommends more widespread experiments on the infection of mosquitoes with wolbachia bacteria to establish the cost of implementation in various geographical locations. This would establish the true cost of implementation thus refining optimal control methods by defining the true value of the cost. Lastly, the study recommends allocation of more resource by both government and non-government entities in the collection of data on the impact of the proposed strategies of controlling the spread of dengue fever in Kenya to enhance improved public health outcomes.

Author contributions: Conceptualization, BN; methodology, BN; software, BN; validation, BN, GK and MW; formal analysis, BN; investigation, BN; resources, BN; data curation, BN; writing—original draft preparation, BN; writing—review and editing, BN; visualization, BN; supervision, GK and MW; project administration, GK and MW; funding acquisition, BN. All authors have read and agreed to the published version of the manuscript.

Conflict of interest: The authors declare no conflict of interest.

References

1. Nyanaro B, Kimathi G, Wainaina M. Mathematical modelling of dengue fever transmission dynamics in kenya. Journal of AppliedMath. 2024; 2(5): 1807–1807.
2. Muthanje EM, Kimita G, Nyataya J, et al. March 2019 dengue fever outbreak at the kenyan south coast involving dengue virus serotype 3, genotypes iii and v. PLOS Global Public Health. 2022; 2(3): e0000122.
3. Bosire C, Mutuku F, Ndenga B, et al. A narrative review of dengue fever infection and epidemic activity in kenya (2010 to 2020). PAMJ One Health. 2023; 12(10): 2023.
4. Mwanyika GO, Moir M, Musa AO, et al. A decade of dengue disease burden in africa (2013–2023): A systematic review. medRxiv. 2024. doi: 10.1101/2024.10.22.24315827

5. Xue L, Ren X, Magpantay F, et al. Optimal control of mitigation strategies for dengue virus transmission. Bulletin of Mathematical Biology. 2021; 83: 1–28.
6. Kairu A, Were V, Isaaka L, et al. Modelling the cost-effectiveness of essential and advanced critical care for covid-19 patients in kenya. BMJ global health. 2021; 6(12): e007168.
7. Rajendran D, Vinayagam S, Sekar K, et al. Symbiotic bacteria: Wolbachia, midgut microbiota in mosquitoes and their importance for vector prevention strategies. Microbial Ecology. 2024; 87(1): 154.
8. Hamed AMR, El-Sherbini MS, Abdeltawab MSA. Eco-friendly mosquito-control strategies: Advantages and disadvantages. Egyptian Academic Journal of Biological Sciences, E. Medical Entomology & Parasitology. 2022; 14(1): 17–31.
9. Khan MA, Fatmawati. Dengue infection modeling and its optimal control analysis in east java, indonesia. Heliyon. 2021; 7(1): e06023.
10. Zou L, Chen J, Feng X, Ruan S. Analysis of a dengue model with vertical transmission and application to the 2014 dengue outbreak in guangdong province, china. Bulletin of Mathematical Biology. 2018; 80: 2633–2651.
11. Asamoah JKK, Yankson E, Okyere E, et al. Optimal control and cost-effectiveness analysis for dengue fever model with asymptomatic and partial immune individuals. Results in Physics. 2021; 31: 104919.
12. Ma C, Li X, Zhao Z, et al. Understanding dynamics of pandemic models to support predictions of covid-19 transmission: Parameter sensitivity analysis of sir-type models. IEEE Journal of Biomedical and Health Informatics. 2022; 26(6): 2458–2468.
13. Khan AA, Ullah S, Amin R. Optimal control analysis of covid-19 vaccine epidemic model: A case study. The European Physical Journal Plus. 2022; 137(1): 1–25.
14. Kumari N, Kumar S, Sharma S, et al. Basic reproduction number estimation and forecasting of covid-19: A case study of india, brazil and peru. Communications on Pure & Applied Analysis. 2023; 22(2).
15. Chan M, Johansson MA. The incubation periods of dengue viruses. PloS one. 2012; 7(11): e50972.
16. Osman S, Makinde OD. A mathematical model for coinfection of listeriosis and anthrax diseases. International Journal of Mathematics and Mathematical Sciences. 2018; 2018(1): 1725671.
17. Osman S, Otoo D, Sebil C. Analysis of listeriosis transmission dynamics with optimal control. Applied Mathematics. 2020; 11(7): 712–737.
18. Osman S, Otoo D, Makinde OD. Modeling anthrax with optimal control and cost effectiveness analysis. Applied Mathematics. 2020; 11(3): 255–275.
19. Lee JS, Mogasale V, Lim JK, et al. A multi-country study of the economic burden of dengue fever based on patient-specific field surveys in burkina faso, kenya, and cambodia. PLoS Neglected Tropical Diseases. 2019; 13(2): e0007164.
20. Cohen J, Dupas P. Free distribution or cost-sharing? Evidence from a malaria prevention experiment in kenya. The Quarterly Journal of Economics. 2010; 125(1): 1–45.
21. Knerer G, Currie CSM, Brailsford SC. The economic impact and cost-effectiveness of combined vector-control and dengue vaccination strategies in thailand: Results from a dynamic transmission model. PLOS Neglected Tropical Diseases. 2020; 14(10): e0008805.